Author version: *J. Acoust. Soc. Am., vol.136(4); 2014; 1972-1981*

Multifractal detrended fluctuation analysis to characterize phase couplings in seahorse (*Hippocampus kuda*) feeding clicks

K. Haris[1,a)] , Bishwajit Chakraborty[1], A. Menezes[1], R. A. Sreepada[1], W. A. Fernandes[1]

[1]CSIR-National Institute of Oceanography, Dona Paula, Goa 403004, India

Abstract: Nonlinear phenomena in animal vocalizations fundamentally includes known features, namely, frequency jump, subharmonics, biphonation and chaos. In the present study, the multifractal detrended fluctuation analysis (MFDFA) has been employed to characterize the phase couplings revealed in the feeding clicks of *Hippocampus kuda* yellow seahorse. The fluctuation function $F_q(s)$, generalized Hurst exponent $h(q)$, multifractal scaling exponent $\tau(q)$ and the multifractal spectrum $f(\alpha)$ calculated in the procedure followed were analyzed to comprehend the underlying nonlinearities in the seahorse clicks. The analyses carried out reveal long-range power-law correlation properties in the data, substantiating the multifractal behavior. The resulting $h(q)$ spectrum exhibits a distinct characteristic pattern in relation to the seahorse sex and size, and reveals a spectral *blind spot* in the data that was not possible to detect by conventional spectral analyses. The corresponding multifractal spectrum related shape parameter $\Delta h(q)$ is well clustered, defining the individual seahorse clicks. The highest degree of multifractality is evident in the 18 cm male seahorse, signifying greater heterogeneity. A further comparison between the seahorse body size and weight (wet) with respect to the shape parameter $\Delta h(q)$ and the second-order Hurst exponent $h(q=2)$ underscores the versatility of MFDFA as a robust statistical tool to analyze bioacoustic observations.

PACS number(s): 43.80.Ka, 43.25.Ts, 43.25.Rq

[a)] Electronic mail: K. Haris (harihassainar@gmail.com)

I. INTRODUCTION

The framework of *nonlinear phenomena* (NLP) from the physics discipline is now being used to explain bioacoustic observations (Wilden *et al*., 1998) including species characterization. The NLP is rooted in the intrinsic nonlinear oscillations of the acoustic signal generated during the sound production. Four major types of NLP have been documented, as can be gleaned from different seminal scientific literature (Wilden *et al*., 1998; Fitch *et al*., 2002). (i) Frequency jump: a signal spectrum comprises of a fundamental frequency f_0, and the frequency jump represents a break in the f_0 with abrupt and discontinuous increase or decrease in the vibration rate. (ii) Subharmonics: the additional intermediate spectral components that appear in the harmonic stack, typically at integer fractions of the fundamental frequency f_0 (i.e., $f_0/2$, $f_0/3$). (iii) Biphonation: the simultaneous occurrence of two independent fundamental frequencies. (iv) Chaos: a broadband frequency segment with no particular harmonics in a signal spectrum (Schneider and Anderson, 2011).

NLP are common in human (Mende *et al*., 1990; Herzel *et al*., 1995; Wilden *et al*., 1998; Tokuda *et al*., 2007) and in animal vocalizations, particularly among: (i) Mammalians [common chimpanzee (Riede *et al*., 2004, 2007), rhesus macaque (Fitch *et al*., 2002), meerkat (Townsend and Manser, 2011), corsican red deer (Facchini *et al*., 2003), dog (Riede *et al*., 2000; Tokuda *et al*., 2002; Volodina *et al*., 2006), red wolf (Schneider and Anderson, 2011), whale (Tyson *et al*., 2007) and manatee (Mann *et al*., 2006)]. (ii) Aves [cockatoo (Fletcher, 2000), magpie (Suthers *et al*., 2011), zebra finch (Fee *et al*., 1998) and northern mockingbird (Zollinger *et al*., 2008)]. (iii) Reptiles [crocodile (Benko and Perc, 2009)], Pisces [fish (Rice *et al*., 2011)], Amphibians [frog (Feng *et al*., 2009)] and Insects [cicada (Hughes *et al*., 2009)].

In the present study, nonetheless, the feeding clicks of seahorse *Hippocampus kuda* (*H. kuda*) belonging to the family Syngnathidae are recorded in a captive environment. Seahorses typically generate stridulatory sounds, akin to the sound of snapping fingers, in a variety of circumstances, e.g., during feeding, courtship and copulation, induction of the seahorse to a new environment and inter-male competition (Colson *et al*., 1998; Anderson, 2009; Chakraborty *et al*., 2014b). The recorded feeding clicks of *H. kuda* are analyzed to characterize the phase couplings [depicted in Fig. 1(b)] across temporal scales that generate the intermittency in the data. The phase couplings generated by a nonlinear processes can be fundamentally differentiated by estimating Lyapunov exponents (as in Fletcher, 2000;

Facchini *et al*., 2003; Mann *et al*., 2006; Tyson *et al*., 2007; Benko and Perc, 2009) or fractal exponents (Loutridis, 2009). Accordingly, considering the latter aspect, the present work carryout multifractal detrended fluctuation analysis (MFDFA) (Kantelhardt *et al*., 2002; Ihlen, 2012) to characterize the phase couplings revealed in the feeding clicks of *H. kuda* yellow seahorse. The multifractal analyses followed herein is a robust technique to identify the scaling behavior and uncover the spectral *blind spot* (Mandelbrot, 1997) in the seahorse feeding clicks that was not viable by conventional spectral analyses. This is an innovative application used in several other fields including: sound-field diffuseness (Loutridis, 2009), music sequences (Su and Wu, 2006; Telesca and Lovallo, 2011) and human heart beat dynamics (Ivanov *et al*., 1999; Goldberger *et al*., 2002; Gierałtowski *et al*., 2012).

The remaining part of this presentation is organized as follows. Section II describes recording of seahorse feeding clicks in a controlled laboratory environment, followed by the signal processing methodology. A brief theoretical overview of MFDFA is also recapped in this section. Section III interprets the multifractal spectrum related shape parameter in terms of seahorse sex and size, followed by concluding remarks in Sec. IV.

II. MATERIALS AND METHODS

A. Seahorse feeding click recording

Hydrophone (C55 M/s Cetacean Research Technology, Seattle, USA) having 20 dB pre-amplifier gain and receiving sensitivity of –185 dB re 1 V μPa^{-1} was used for sound recordings. The hydrophone was connected to an analog-to-digital (A/D) converter installed in a personal computer (PC). The digital data were transferred to the PC via a parallel port interface at a sampling frequency of 10 kHz (Chakraborty *et al*., 2014b). The passive acoustic recordings were carried out in the aquaculture laboratory complex of CSIR-National Institute of Oceanography, India, where the techniques for standardization of captive breeding, rearing and culture of seahorse species are being established (Pawar *et al*., 2011). Various seahorse husbandry practices as described in Pawar *et al*. (2011) were followed prior to the experiment.

The hydrophone was kept immersed in a glass tank containing aerated fresh seawater, up to a depth of 30 cm from the surface. The hydrophone was placed around 60 cm away from the seahorse. The tank was kept over 40 mm thick flexible foam to reduce mechanical, electrical and background noise. This setup was retained during the course of the experiment. The seahorses were generally fed thrice a day

with different live prey organisms namely, copepodites, *Artemia nauplii* and mysids (*Mesopodopsis orientalis*). The seahorse feed (mysids) were placed in the tank, and the clicks were recorded commencing at 14:00 hr. A total of twenty seahorse feeding clicks corresponding to 12 cm female, 12 cm male, 16 cm male, and 18 cm male were recorded and analyzed in the study. The oscillogram and spectrogram of 12 cm female seahorse click are shown as typical examples [Figs. 1(a), 1(b)] to illustrate the complexities and phase couplings in the signal.

B. Noise removal and signal extraction

The extraction of noise-free clicks is imperative prior to carrying out the MFDFA. The presence of background noise in the analyses generates spurious and erroneous multifractality (Ludescher *et al*., 2011; Gulich and Zunino, 2012). Accordingly, the time duration (precise start- and end-points) of the clicks were identified employing a three step procedure as illustrated in the Fig. 2. The low frequency periodic artifact (mainly due to electrical noise) is inevitable in the laboratory-based observational passive acoustic records. Therefore, it was necessary to select a cut-off frequency (high pass filter) to discard the low frequency artifacts in the raw data stream. At the initial step, the low frequency background noise in the raw data was eliminated by defining a cut-off frequency of 1 kHz. The seahorse clicks analyzed in the study were evidently of high frequency (>1 kHz) signals (Chakraborty *et al*., 2014b) [Fig. 1(b)] and the filtering procedure adopted here can eliminate the periodic low frequency trends in the data to improve the MFDFA. A representative data stream after filtering is shown in Figs. 1a, 2a.

The start-point of the click (after filtering) is conspicuous as seen in Fig. 2b, whereas the end-point identification is convoluted because the subtle difference in amplitude levels of damping signal and the noise renders it visually undetectable. Consequently, in the second step, a noise level reduction method was performed by multiplying the time series x_k with ratios of its corresponding absolutes $|x_k|$ to the maximum absolute value $[x_k|x_k|/\max|x_k|]$. This procedure can enhance the contrast between the signal and background noise in the data stream. The first-difference of the resulting time series was subsequently computed [Fig. 2(c)] to facilitate the envelope detection procedure. In the final step Hilbert transform-based envelope detection procedure (Zimmer, 2011) was utilized to identify the time duration of the detected signal. After identifying the time window [Fig. 2(d), dash line], the corresponding

amplitude values of each click were extracted from the data stream [depicted in Fig. 2(a)]. The extracted clicks of individual seahorse representing different sex and size were subject to the MFDFA.

C. MFDFA-theoretical overview

A brief theoretical overview of the MFDFA is summarized in this section (Kantelhardt *et al*., 2002; Ihlen, 2012). The general MFDFA is comprised of five major steps. The first step involves the subtraction of the mean $\langle x \rangle$ from the seahorse click time series x_k of length N to determine the cumulated data series $Y(i)$ as:

$$Y(i) \equiv \sum_{k=1}^{i} [x_k - \langle x \rangle], \qquad i = 1,..., N \tag{1}$$

where $\langle x \rangle = (\sum_{k=1}^{i} x_k)/N$. In the second step the resulting profile $Y(i)$ was divided into non-overlapping segments [$N_s \equiv \text{int}(N/s)$] of equal length s.

The local trend for each of the segment was calculated in the third step by a least-square fit of the series to determine the variance

$$F^2(s,v) \equiv \frac{1}{s} \sum_{i=1}^{s} \{Y[(v-1)s + i] - y_v(i)\}^2 \tag{2}$$

for each segment $v = 1,..., N_s$. Here $y_v(i)$ is the fitting polynomial in segment v. Linear, quadratic, cubic or higher order polynomials can also be used in the fitting procedure.

In the fourth step the average over all segments was computed to obtain the q^{th} order fluctuation function

$$F_q(s) \equiv \left\{ \frac{1}{N_s} \sum_{v=1}^{N_s} [F^2(s,v)]^{q/2} \right\}^{1/q}, \tag{3}$$

where the index variable q can take any real value except zero.

The generalized q dependent fluctuation functions $F_q(s)$ depend on the time scale s for different values of q [–5 to 5]. The scaling behavior of the fluctuation function was determined in the fifth step

by estimating the slopes of the plot $\log_2[F_q(s)]$ versus s for each value of q [Fig. 3(a)]. If the series x_k has long-range power-law correlations, $F_q(s)$ scales with s as:

$$F_q(s) \sim s^{h(q)}. \tag{4}$$

The function $h(q)$ is termed as generalized Hurst exponent. Ideally, in the case of a monofractal time series, $h(q)$ is independent of q as the scaling behavior of the variances $F^2(s,v)$ is identical in all the segments v. The averaging procedure in Eq. (3) for a monofractal time series results in identical scaling behavior with different values of q. The function $h(q)$ for positive and negative values of q describes the scaling behavior of the segments with large and small fluctuations respectively.

The $h(q)$ defined in Eq. (4) is directly related to the classical multifractal scaling exponents $\tau(q)$ defined by the standard partition function-based multifractal formalism. The analytical relation between these two sets of multifractal scaling exponents can be represented as:

$$\tau(q) = qh(q) - 1. \tag{5}$$

Another way to characterize a multifractal series is the singularity spectrum $f(\alpha)$ that is related to $\tau(q)$ via a Legendre transform (Kantelhardt *et al.*, 2002),

$$\alpha = \tau'(q) \text{ and } f(\alpha) = q\alpha - \tau(q). \tag{6}$$

Here, α is the singularity strength or Hölder exponent, while $f(\alpha)$ denotes the dimension of the subset of the series characterized by α. Using Eq. (5), it is also possible to directly relate α and $f(\alpha)$ to $h(q)$ as:

$$\alpha = h(q) + qh'(q) \text{ and } f(\alpha) = q[\alpha - h(q)] + 1. \tag{7}$$

1. Description of the multifractal spectrum

In this work we focus on the particulars of the generalized Hurst exponent $h(q)$ spectrum to quantify the multifractal properties of the seahorse feeding click time series. The $h(q)$ and $f(\alpha)$ are mathematically related by the Legendre transformation [Eq. (6)]. Hence, only the results of $h(q)$ curves are considered. The feeding clicks can also be realized as multifractal when the graph of α versus $f(\alpha)$ (multifractal spectrum) exist and has the shape of an inverted parabola (as in Chakraborty *et al.*,

2014a). If the $f(\alpha)$ curve converges to a single point, it can be termed as monofractal wherein the generalized Hurst exponent $h(q)$ is constant for all values of q [Figs. 1(c), 1(d)]. The width of the $h(q)$ curve [$\Delta h(q) = h(q)_{\max} - h(q)_{\min}$] is a measure of multifractality, and indicates the deviation from monofractal behavior. The illustrations of the shape parameters that can be used to describe the multifractality are shown in Figs. 3b, 3d.

In order to distinguish the multifractal spectrum $f(\alpha)$ quantitatively, it is also convenient to compute the width of the spectrum W [$\alpha_{\max} - \alpha_{\min}$] so as to evaluate the overall variability [Fig. 3(d)]. A wider $f(\alpha)$ spectrum is indicative of larger W, signifying multifractality. The width W would be small and tending to zero in the case of a monofractal series. Moreover, the monofractal time series has exponents $\tau(q)$ with a linear q-dependency [Fig. 3(c)], resulting in a stable $h(q)$ [Fig. 1(c)]. The unvarying $h(q)$ reduces the $f(\alpha)$ spectrum to a narrow arc in the monofractal series [Fig. 1(d)]. Conversely, the multifractal time series has $\tau(q)$ with a curved q-dependency [Fig. 3(c)] and a decreasing $h(q)$ (Ihlen, 2012). The multifractal spectrum in such an instance is a wide arc indicating higher multifractality in the data.

III. RESULTS AND DISCUSSION

The MFDFA followed herein has several advantages over the standard power spectral density (PSD) analyses, because it reveals scaling behavior and long-range power-law correlation properties in the data. Previous analyses by Chakraborty *et al.* (2014b) have focused on the quantification of single power-law exponent β (i.e., monofractal feature) to characterize the seahorse clicks. On the other hand, results of the present study affirm that the clicks are intrinsically complex and require multiple exponents for its characterization. Moreover, the β exponent derived from the PSD is implausible as the Fourier analyses require the stationarity of the data (Goldberger *et al.*, 2002). Normally the stationarity requirement is seldom met in the analyzed data. The following section describe the particulars of $h(q)$ spectrum to validate the apparent multifractal properties in the seahorse feeding clicks. The resulting shape parameters [illustrated in Fig. 3(b)] have been statistically analyzed and compared with respect to the seahorse body size and weight (wet).

A. Validation of nonlinearities in feeding clicks

MFDFA can provide satisfactorily good results when the input signals (seahorse click) are noise like time series. The time series can be realized as noise like if the Hurst exponent H varies between 0.2–0.8. The MFDFA can be employed directly in such instances without transforming the signal (Ihlen, 2012). However, the H values of seahorse clicks analyzed in the present study were evidently restricted to H<0.2 [see the inset in Fig. 1(a)]. As suggested by Ihlen (2012), the time series should be integrated before performing MFDFA, and a constant –1 should be added to the resulting parameters $h(q)$, $\tau(q)$ and α.

As mentioned in Section II, the computed $\Delta h(q)$ [Fig. 3(b)] values can be interpreted as a measure of multifractality and nonlinearity in the data. It is important to validate that the resulting $\Delta h(q)$ values are actually generated due to nonlinearities in the data and not from the mere presence of $1/f^{\beta}$ power law and a non-Gaussian probability density function. This validation is possible by performing MFDFA on surrogate series corresponding to each of the feeding clicks (as in Ihlen and Vereijken, 2010). The surrogate series of the feeding clicks were generated employing iterated amplitude adjusted Fourier transformation (IAAFT) (Schreiber and Schmitz, 1996) within a maximum limit of 500 iterations. The IAAFT surrogates replicate the power spectral density and the probability distribution (i.e., statistical properties) of the feeding clicks, but eliminate the phase couplings between the temporal scales (i.e., frequencies). The significant influence of nonlinearities (i.e., phase couplings across temporal scales) in the data can be realized if $\Delta h(q)$ of surrogates have smaller values as compared to the original time series.

The ensemble average of the $h(q)$ values (18 cm male) corresponding to the feeding clicks and associated surrogates reveal significant dominance of nonlinearities in the data [Fig. 4(a)]. Similarly, the distinctly observed differences in $\Delta h(q)$ vales (Fig. 5), corresponding to the data and surrogates further substantiate the observed nonlinearities. Therefore, the juxtaposition of MFDFA and the surrogate test is advantageous to uncover the substantial influence of phase couplings across temporal scales that generate the intermittency (i.e., burstiness) in the seahorse feeding clicks. Moreover, the generalized Hurst exponent spectrum width $\Delta h(q)$ reproduced by the IAAFT surrogates is predominantly influenced

by the attributes of power spectral density and the non-Gaussian probability distribution of the feeding clicks, and not by intrinsic nonlinearities evident in the data.

B. Frequency range characteristic of seahorse feeding clicks

The seahorse clicks were studied for several objectives namely: to understand the effect of induction of the seahorse to a new environment, courtship and copulation (Fish and Mowbray, 1970), behavior and physiology in captive environment (Anderson, 2009) and during feeding (Colson *et al*., 1998; Anderson, 2009; Chakraborty *et al*., 2014b). Emphasizing on the feeding behavior, Colson *et al*. (1998) had conducted a detailed study to substantiate the stridulation hypothesis of sound production, using a novel combination of kinematic, surgical, acoustic and morphological analyses. The stridulation mechanism (i.e., an act of producing sound by rubbing certain body parts together) involves the articulation of two bones in the head (namely, the supraoccipital and the coronet).

The frequency range characteristic of seahorse clicks differ considerably as can be gleaned from different scientific literature. Fish (1953) documented broadband signals (0–4.8 kHz) in *H. hudsonius*, with maximum energy between 300–600 Hz and 400–800 Hz. Colson *et al*. (1998) reported the frequency range of *H. zosterae* and *H. erectus* between 2.65–3.43 kHz and 1.96–2.35 kHz respectively. Anderson (2009) however considered the bandwidth of 0–1 kHz as the prospective range to examine the clicks of *H. erectus*. The frequency range of *H. kuda* analyzed in the present study is consistent with the observations reported by Colson *et al*. (1998). The spectrogram analyses appropriately reveal high frequency (>1 kHz) feeding clicks in *H. kuda* (Chakraborty *et al*., 2014b) [Fig. 1(b)]. The intrinsic complexity of the clicks essentially necessitates the application of the MFDFA to characterize the phase couplings across temporal scales in the data.

C. Particulars of generalized Hurst exponent $h(q)$ spectrum

Twenty seahorse feeding clicks corresponding to 12 cm female, 12 cm male, 16 cm male and 18 cm male were analyzed in the study. The curves of the generalized Hurst exponent $h(q)$ can be realized as a distinct characteristic of a fractal time series. The variations in $h(q)$ spectrum principally account for the underlying fractal organization in a complex signal. The heterogeneity in the click is visually evident [in Fig. 2(b)] and the $h(q)$ spectrum analyzed herein quantitatively determines the scaling properties of

the data. The ensemble average of the $h(q)$ values (q ranging between –5 to 5) corresponding to the individual seahorse further reveals the apparent multifractal behavior of the feeding clicks [Fig. 4(b)].

The markedly observed multifractality in the clicks also indicate dissimilarities in scaling behavior of the segments v with small and large fluctuations. There will be significant dependence of $h(q)$ on q if small and large fluctuations in the segments are different (Kantelhardt *et al.*, 2002). Indeed, for positive q values, the segments v with large variance $F^2(s,v)$ [in Eq. (2)] will dominate the average $F_q(s)$ [in Eq. (3)]. The resulting $h(q)$ values describe the scaling of segments with large fluctuations. The large fluctuations in the clicks are usually characterized by the smaller scaling exponent $h(q)$ [Fig. 4(b)]. Conversely, for negative q values, the segments with small variance $F^2(s,v)$ will dominate the average $F_q(s)$. The corresponding $h(q)$ values emphasize the scaling behavior of segments with small fluctuations. Usually small fluctuations are characterized by larger scaling exponent $h(q)$. Correspondingly, the $h(q)$ spectrum related analyses of the individual seahorse reveal different scaling behavior associated with small fluctuations. Whereas, the differences in the scaling behavior of large fluctuations correspond to individual seahorse clicks, are meager [Fig. 4(b)]. Therefore, the differences in long-range correlation properties present in the clicks can be mainly attributed to the scaling behavior due to small fluctuations.

In a multifractal seahorse click, the intermittent periods with large and small fluctuations generate a decreasing $h(q)$ [Fig. 4(b)]. The decreasing $h(q)$ indicate that the segments with small fluctuations have a random walk like structure, whereas segments with large fluctuations resemble a noise structure (Ihlen, 2012). The unvarying $h(q)$ on the contrary signifies a homogeneous structure with monofractality. With a relatively small $\Delta h(q)$ value of 0.073, the $h(q)$ spectrum analyzed in the present study reveals a non-multifractality in the background noise [Fig. 1(c)]. As mentioned earlier, the degree of multifractality can be easily related to the width of the generalized Hurst exponent spectrum $\Delta h(q)$ [Fig. 3(b)]. The $\Delta h(q)$ values calculated for the individual seahorse clicks are shown in Fig. 5. The range of $\Delta h(q)$ values varies between: 0.319–0.439, 0.592–0.613, 0.704–0.752, and 0.896–1.101, respectively for the 16 cm male, 12 cm male, 12 cm female, and 18 cm male. The detailed $\Delta h(q)$ values are summarized in Table I. In order to compare the $h(q)$ spectrum quantitatively, it is convenient to

calculate the ensemble average of the $h(q)$ values that correspond to the individual seahorse. The resulting width values $\Delta h(q)$ get successively reduced from maximum to minimum: 0.983, 0.734, 0.603, and 0.380, associated with 18 cm male, 12 cm female, 12 cm male, and 16 cm male respectively [Fig. 4(b)]. Such reduction in $\Delta h(q)$ values indicate decrease in the degree of multifractality. The highest degree of multifractality is evident in the 18 cm male seahorse, signifying greater heterogeneity. The low $\Delta h(q)$ value of 16 cm male indicates relatively reduced multifractality and heterogeneity as compared to the values of the remaining seahorses. All the seahorses possess a characteristic different $h(q)$ curve and a $\Delta h(q)$ value in relation to its sex and size, permitting individual identification.

The $h(q)$ spectrum related analyses further suggest that the variability of the feeding clicks in the individual seahorse is distributed according to the power-law (Chakraborty *et al*., 2014b). The computed exponents characterizing the power-law behavior differentiate the irregular sound signals among the individual in terms of its sex and size [Fig. 4(b)]. The quantitative characterization of the feeding clicks based on the MFDFA is a novel approach to analyze the nonlinearities (i.e., phase couplings across temporal scales) in the data. However, it is important to note that the performance of the MFDFA based on the signal time series is significantly affected by the presence of background noise in the data (Ludescher *et al*., 2011; Gulich and Zunino, 2012). Therefore, it is imperative to eliminate the background noise and periodic artifacts in the data, before the analyses is performed.

D. Comparison of $\Delta h(q)$ with respect to seahorse body size and weight

The variability of the multifractal spectrum related shape parameter $\Delta h(q)$ in the seahorse feeding clicks can be related to the interpretation of complexities in: sound-field diffuseness (Loutridis, 2009), music sequences (Su and Wu, 2006; Telesca and Lovallo, 2011) and human heart beat dynamics (Ivanov *et al*., 1999; Goldberger *et al*., 2002; Gierałtowski *et al*., 2012). The above referred multifractality aspects support the fact that wider the spectrum width, higher would be the irregularity. The wider $h(q)$ spectrum in the 18 cm male seahorse reflects a broader variation in the amplitude values, implying greater heterogeneity and nonlinearity. Comparison between the seahorse body size and weight (wet) with respect to the computed shape parameter further evidences the individual characteristics. The scatter diagram reveals four major clustering patterns designating individual seahorse clicks [Fig. 6(a)].

The animal vocalizations are frequently characterized by two basic parameters, namely the dominant and peak frequency. Colson *et al*. (1998) and Chakraborty *et al*. (2014b) had compared the peak frequency derived from the seahorse feeding clicks with respect to its body size, weight and sex. The corresponding correlation coefficients of the peak frequency versus body size and weight of the seahorse were found to be meager and subtle (see Fig. 8 in Chakraborty *et al*., 2014b). The reason for such a subtle correlation may be ascribable to the observed phase couplings across temporal scales in the feeding clicks [Fig. 1(b)]. The phase coupling behavior substantially convolutes the detection of the peak frequencies in the data. Each of the clicks has a broad power spectrum with many subsidiary peaks. This can be corroborated by the spectrogram analyses provided in the Fig. 1b. The power spectrum also encompass several dominant frequencies, which presumably represent major oscillation modes in the feeding clicks, but the amplitudes of these modes vary in a complex manner (Wilden *et al*., 1998; Fletcher, 2000). The phase couplings generated by a nonlinear processes can be comprehended by examining the underlying differential equations in a physical system. In the biological system (with seahorse) such an approach is not viable. Alternatively, the nature of the underlying equations can be examined by analyzing the sound output (Fletcher, 2000), because the seahorse click retains an irregular structure with a definite and repetitive pattern. Accordingly, emphasizing on the self-similarity of the feeding clicks, it is convenient to analyze the signal by estimating the associated multifractal exponents. The resulting multifractal spectrum of seahorses, possess characteristically different $\Delta h(q)$ values in relation to its weight and size [Fig. 6(a)].

E. Limitation of traditional techniques and MFDFA

The power spectrum that account for the relative frequency content of a signal has been widely applied to characterize correlations in a time series. The power spectral density analyses require data in stationary form, and its application to nonstationary time series can lead to spurious results. As mentioned in Ihlen and Vereijken (2010), the time series can be decomposed into a sum of oscillations with wavelength $\Delta t = 1/f^{\beta}$ to characterize the presence of $1/f^{\beta}$ power law. This decomposition is typically performed by Fourier transformation. The Fourier transformation basically assumes that the amplitude $A_{\Delta t}$ of each oscillation is independent to each other (see Fig.1a in Ihlen and Vereijken, 2010). This fundamental assumption is violated due to the presence of intermittency generated by the small and large fluctuations in the seahorse feeding clicks. These intermittent fluctuations in the feeding clicks

further imply an inhomogeneous distribution, and therefore leads to a time dependency in both the probability density function and spectral exponent β.

The conventional analyses tools of both $1/f^{\beta}$ power law and the non-Gaussian probability density function used to characterize seahorse feeding clicks assume that the spectral exponent β is homogeneous in time. As a consequence, these analyses tools are blind to the presence of intermittency in the feeding clicks. The intermittency in seahorse feeding clicks can be viewed as an inherent property that is implausible to be quantified by a single exponent β, and lies within the *blind spots* (Mandelbrot, 1997) of the Fourier lens (Ihlen and Vereijken, 2010).

To illustrate the spectral *blind spot*, the ensemble average of the $h(q)$ values corresponding to the individual seahorse is exemplified in Fig. 4b. Normally, the exponent $h(q)$ will depend on q. For q=2, the Hurst exponent H in standard detrended fluctuation analyses (DFA) is retrieved. The computed H value account for the overall root-mean-square (RMS) fluctuations in the data and also represents the spectral exponent β. Apparently, the intercept point of the $h(q)$ curves corresponding to individual seahorse is close to q=2 [Fig. 4(b)]. This intercept pattern demonstrates a spectral *blind spot* detected by MFDFA, and resulting in identical and subtle variations in the spectral exponent β [Fig. 6(b)]. Therefore, the MFDFA adopted in the present study can quantitatively distinguish the intermittent fluctuations in the individual seahorse clicks that is not possible by conventional spectral analyses.

F. Biological implications

The concept of NLP in bioacoustics was first introduced by Wilden *et al.* (1998) to quantify the complexities in animal vocalizations. The NLP has been hypothesized to take on an important role in individual identification, animal size description and health status of a given animal (Fitch *et al.*, 2002). Riede *et al.* (2004) documented three hypothesized NLP functions that were applicable to chimpanzee pant hoots; (i) NLP can be used to determine the individual's vocal distinctiveness (Wilden *et al.*, 1998; Volodina *et al.*, 2006; Feng *et al.*, 2009); that could help in identifying the signaling effectiveness of a seahorse, (ii) NLP can also function to distinguish the auditory impact of animal calls (Riede *et al.*, 2007); which in the case of seahorses could be purposeful for attracting mates as well as for signaling their status or physical condition. If that be the case, Riede *et al.* (2004) suggested that the individuals

can enhance the number of NLP in order to maximize the impact of their signals, (iii) the existence of NLP could function as a cue of an individual's health and physical condition.

As mentioned in the introduction, seahorses typically generate stridulatory sounds in a variety of circumstances (e.g., during feeding, courtship and copulation, induction of the seahorse to a new environment and inter-male competition). A seahorse may evaluate clicks produced by nearby seahorses to differentiate between mates and non-mates (Vincent and Sadler, 1995). Likewise, the clicks associated with feeding strikes could be an indication of a food source to a monogamous mate as a strategy for increasing a mate's reproductive fitness (Anderson, 2009). Anderson *et al*. (2011) had used the lined seahorse (*H. erectus*) to assess the effect of chronic aquarium noise exposure to fish health and stress. The stress is connected to various physiological and behavioral functions, and can effect suppression of immune function, growth rate and reproduction. A complete assessment of behavioral functions (Popper and Carlson, 1998) is beyond the scope of present investigation, and further studies are required to relate the role of observed NLP with the behavior and biomechanical aspects of a feeding seahorse. In the present study, we posit that much complexity is evident in seahorse feeding clicks resulting from nonlinearities in the production system, signifying that a rather simple neural command to the supraoccipital and the coronet bones in the seahorse head (Colson et *al*., 1998) can contribute to a highly complex and individually variable acoustic signal. A more definitive evidence can be sought by advancing this work, by increasing the number of samples from individuals including behavioral observations.

The occurrence and characteristics of NLP must be documented prior to examining the role of suggested functions in a given animal. The NLP has been overlooked in traditional analyses due to the lack of adequate conceptual framework and appropriate tools for analyses. The tools typically used by bioacousticians, such as power spectral and spectrogram analyses are not suitable to characterize signals generated by a nonlinear system (implying that the equations that govern the nonlinearity in sound production might include squared, cubed or higher-order moments). This approach is less meaningful in bioacoustics, necessitating the development of robust mathematical tools for analyzing nonlinear systems. Significantly, MFDFA can distinguish the intermittency (and phase couplings) in seahorse feeding clicks, and can be used to analyze similar patterns observed in other species as well.

IV. CONCLUDING REMARKS

The multifractal properties of the seahorse feeding clicks have been investigated by applying multifractal detrended fluctuation analysis (MFDFA). The fluctuation function $F_q(s)$, generalized Hurst exponent $h(q)$, multifractal scaling exponent $\tau(q)$ and the multifractal spectrum $f(\alpha)$ associated with individual seahorse clicks have been calculated in the procedure followed. The preliminary results obtained by applying the MFDFA in the field of bioacoustics provide experimental evidence of multifractality. The multifractal behavior can be attributed to the fluctuations in the scaling properties of the feeding clicks and can be also explained by the following findings:

- The seahorse clicks are intrinsically complex and display non-equilibrium fluctuations that cannot be analyzed accurately with standard methods, including power spectral density (PSD) analyses. The observed nonlinearities (i.e., phase couplings across temporal scales) in such data calls for the application of MFDFA (adapted from modern statistical physics) to characterize the underlying self-similarity evident in the feeding clicks.
- The MFDFA has the potential to analyze nonstationary feeding click time series revealing the presence of long-range power-law correlation properties in the data. The long-range power-law correlations indicate that broad ranges of scaling exponents are required to describe the complexity.
- The outcome of MFDFA, the $h(q)$ spectrum and related shape parameter $\Delta h(q)$ reveals multifractal character in the individual seahorse clicks. The high $\Delta h(q)$ value in the 18 cm male seahorse reflects a broader variation in the amplitude values, signifying greater heterogeneity and multifractality. The low $\Delta h(q)$ value of 16 cm male, on the flip side, indicates relatively reduced multifractality and heterogeneity as compared to the properties of the remaining seahorses.
- Further comparison between the seahorse body size and weight (wet) with respect to the computed shape parameter depicts a distinct characteristic $\Delta h(q)$ values in relation to its sex and size, suggesting individual signature.

Considering the diverse applications of multifractal techniques in natural scientific disciplines, this work underscores the versatility of the MFDFA to investigate bioacoustic observations. The MFDFA utilized

in our work is a first-time endeavor to analyze the nonlinearities (i.e., phase couplings across temporal scales) in the seahorse feeding clicks. The present investigation ascertains an important finding, however further studies are required to examine the results with the behavior and biomechanical aspects of a feeding seahorse.

ACKNOWLEDGMENTS

The authors are thankful to Dr. SWA Naqvi, Director, CSIR-NIO, for providing facilities to carry out this study. We are grateful to Espen A.F. Ihlen (Norwegian University of Science and Technology, Norway) for making available the multifractal toolbox in the public domain (http://www.ntnu.edu/inm/geri/software). The MATLAB code used to generate IAAFT surrogate time series was downloaded from the *chaotic systems toolbox* available at http://www.mathworks.in/matlabcentral/fileexchange/1597-chaotic-systems-toolbox. The work of K Haris was supported by the Council of Scientific and Industrial Research (CSIR) through a grant of research fellowship. The authors convey their gratitude to Prof. Arthur N. Popper (Associate Editor), and the reviewers for their meticulous remarks to improve the manuscript.

REFERENCES

Anderson, P. A. (**2009**). The functions of sound production in the lined seahorse, *Hippocampus erectus*, and effects of loud ambient noise on its behavior and physiology in captive environments, PhD Thesis, University of Florida, Gainesville, FL, USA, pp. 1–190.

Anderson, P.A., Berzins, I.K., Fogarty, F., Hamlin, H.J., and Guillete. L. (**2011**). "Sound, stress, and seahorses: The consequences of a noisy environment to animal health," Aquaculture **311**,129–138.

Benko, T. P., and Perc, M. (**2009**). "Nonlinearities in mating sounds of American crocodiles," BioSystems **97**, 154–159.

Chakraborty, B., Haris, K., Latha, G., Maslov, N., and Menezes, A. (**2014a**). "Multifractal approach for seafloor characterization," IEEE Geosci. Remote Sens. Lett. **11**, 54–58.

Chakraborty, B., Saran, A. K., Sinai Kuncolienker, D., Sreepada, R. A., Haris, K., and Fernandes, W. (**2014b**). "Characterization of Yellow Seahorse *Hippocampus kuda* feeding click sound signals in a laboratory environment: an application of probability density function and power spectral density analyses," Bioacoustics **23**, 1–14.

Colson, D. J., Patek, S. N., Brainerd, E. L., and Lewis, S. M. (**1998**). "Sound production during feeding in *Hippocampus* seahorse (Syngnathidae)," Environ. Biol. Fish. **51**,221–229.

dos Santos Lima, G. Z., Corrêa, M. A., Sommer, R. L., and Bohn, F. (**2012**). "Multifractality in domain wall dynamics of a ferromagnetic film," Phys. Rev. E **86**, 066117.

Facchini, A., Bastianoni, S., Marchettini, N., and Rustici, M. (**2003**). "Characterization of chaotic dynamics in the vocalization of *Cervus elaphus corsicanus* (L)," J. Acoust. Soc. Am. **114**, 3040–3043.

Fee, M. S., Shraiman, B., Pesaran, B., and Mitra P. P. (**1998**). ''The role of nonlinear dynamics of the syrinx in the vocalizations of a songbird,'' Nature **395**, 67–71.

Feng, A. S., Riede, T., Arch, V. S., Yu, Z., Xu, Z. -M., Yu, X. -J., and Shen, J. -X. (**2009**). "Diversity of the vocal signals of concave-eared torrent frogs (*Odorrana tormota*): Evidence for individual signatures," Ethology **115**, 1015–1028.

Fish, M. P. (**1953**). "The production of underwater sound by northern seahorse, *Hippocampus hudsonius*," Copeia **1953**, 98–99.

Fish, M. P., and Mowbray, W. H. (**1970**). *Sounds of western North Atlantic fishes: a reference file of biological underwater sounds* (The Johns Hopkins University Press, Baltimore, USA), pp. 1–207.

Fitch, W. T., Neubauer, J., and Herzel, H. (**2002**). "Calls out of chaos: The adaptive significance of nonlinear phenomena in mammalian vocal production," Anim. Behav. **63**, 407–418.

Fletcher, N. H. (**2000**). "A class of chaotic bird calls?," J. Acoust. Soc. Am. **108**, 821–826.

Gierałtowski, J., Zebrowski, J. J., and Baranowski, R. (**2012**). "Multiscale multifractal analysis of heart rate variability recordings with a large number of occurrences of arrhythmia," Phys. Rev. E **85**, 021915.

Goldberger, A. L., Amaral, L. A. N., Hausdorff, J. M., Ivanov, P. Ch., Peng, C. K., and Stanley, H. E. (**2002**). "Fractal dynamics in physiology: Alterations with disease and aging," Proc. Natl. Acad. Sci. U.S.A. **99**, 2466–2472.

Gulich, D., and Zunino, L. (**2012**). "The effects of observational correlated noises on multifractal detrended fluctuation analysis," Physica A **391**, 4100–4110.

Herzel, H., Berry, D. A., Titze, I. R., and Steinecke, I. (**1995**). "Nonlinear dynamics of the voice: signal analysis and biomechanical modeling," Chaos **5**, 30–34.

Hughes, D. R., Nuttall, A. H., Katz, R. A., and Carter, G. C. (**2009**). "Nonlinear acoustics in cicada mating calls enhance sound propagation," J. Acoust. Soc. Am. **125**, 958–967.

Ihlen, E. A. F., and Vereijken, B. (**2010**). "Interaction-dominant dynamics in human cognition: Beyond $1/f^{\alpha}$ fluctuations," J. Exp. Psychol. Gen. **139**, 436–463.

Ihlen, E. A. F. (**2012**). "Introduction to multifractal detrended fluctuation analysis in Matlab," Front. Physiol. **3**, 1–18.

Ivanov, P. Ch., Amaral, L. A. N., Goldberger, A. L., Havlin, S., Rosenblum, M. G., Struzik, Z. R., and Stanley, H. E. (**1999**). "Multifractality in human heartbeat dynamics," Nature **399**, 461–465.

Kantelhardt, J. W., Zschiegner, S. A., Koscielny-Bunde, E., Havlin, S., Bunde, A., and Stanley, H. E. (**2002**). "Multifractal detrended fluctuation analysis of nonstationary time series," Physica A **316**, 87–114.

Loutridis, S. J. (**2009**). "Quantifying sound-field diffuseness in small rooms using multifractals," J. Acoust. Soc. Am. **125**, 1498–1505.

Ludescher, J., Bogachev, M. I., Kantelhardt, J. W., Schumann, A. Y., and Bunde, A. (**2011**). "On spurious and corrupted multifractality: The effects of additive noise, short-term memory and periodic trends," Physica A **390**, 2480–2490.

Mandelbrot, B. B. (**1997**). *Fractals and scaling in finance* (Springer-Verlag, New York, NY, USA), pp. 163–164.

Mann, D. A., O'Shea, T. J., and Nowacek, D. P. (**2006**). "Nonlinear dynamics in manatee vocalizations," Marine Mammal Sci. **22**, 548–555.

Mende, W., Herzel, H., and Wermke, K. (**1990**). ''Bifurcations and chaos in newborn infant cries,'' Phys. Lett. A **145**, 418–424.

Pawar, H. B., Sanaye, S. V., Sreepada, R. A., Harish, V., Suryavanshi, U., Tanu., and Ansari, Z. A. (**2011**). "Comparative efficacy of four anaesthetic agents in the yellow seahorse, *Hippocampus kuda* (Bleeker, 1852)," Aquaculture **311**,155–161.

Popper, A.N., and Carlson, T.J. (**1998**). "Application of sound and other stimuli to control fish behavior," T. Am. Fish. Soc. **127**, 673–707.

Rice, A. N., Land, B. R., and Bass, A. H. (**2011**). "Nonlinear acoustic complexity in a fish 'two-voice' system," Proc. R. Soc. B **278**, 3762–3768.

Riede, T., Arcadi, A. C., and Owren, M. J. (**2007**). "Nonlinear acoustics in the pant hoots of common chimpanzees (*Pan troglodytes*): Vocalizing at the edge," J. Acoust. Soc. Am. **121**, 1758–1767.

Riede, T., Herzel, H., Mehwald, D., Seidner, W., Trumler, E., Tembrock, G., and Böhme, G. (**2000**). ''Nonlinear phenomena in the natural howling of a dog–wolf mix,'' J. Acoust. Soc. Am. **108**, 1435–1442.

Riede, T., Owren, M. J., and Arcadi, A. C. (**2004**). "Nonlinear acoustics in the pant hoot vocalizations of common chimpanzees (*Pan troglodytes*): Frequency jumps, subharmonics, biphonation, and deterministic chaos," Am. J. Primatol. **64**, 277–291.

Schneider, J. N., and Anderson, R. E. (**2011**). "Tonal vocalizations in the red wolf (*Canis rufus*): Potential functions of nonlinear sound production," J. Acoust. Soc. Am. **130**, 2275–2284.

Schreiber, T., and Schmitz, A. (**1996**). "Improved surrogate data for nonlinearity tests," Phys. Rev. Lett. **77**,635–638.

Suthers, R. A., Wild, J. M., and Kaplan, G. (**2011**). "Mechanisms of song production in the Australian magpie," J. Comp. Physiol. A **197**, 45–59.

Su, Z. -Y., and Wu, T. (**2006**). "Multifractal analyses of music sequences," Physica D **221**, 188–194.

Telesca, L., and Lovallo, M. (**2011**). "Revealing competitive behaviours in music by means of the multifractal detrended fluctuation analysis: application to Bach's Sinfonias," Proc. R. Soc. A **467**, 3022–3032.

Tokuda, I. T., Horacek, J., Svec, J. G., and Herzel, H. (**2007**). "Comparison of biomechanical modeling of register transitions and voice instabilities with excised larynx experiments," J. Acoust. Soc. Am. **122**, 519–531.

Tokuda, I. T., Riede, T., Neubauer, J., Owren, M. J., and Herzel, H. (**2002**). "Nonlinear analysis of irregular animal vocalizations," J. Acoust. Soc. Am. **111**, 2908–2919.

Townsend, S. W., and Manser, M. B. (**2011**). "The function of nonlinear phenomena in meerkat alarm calls," Biol. Lett. **7**, 47–49.

Tyson, R. B, Nowacek, D. P., and Miller, P. J. O. (**2007**). "Nonlinear phenomena in the vocalizations of North Atlantic right whales (*Eubalaena glacialis*) and killer whales (*Orcinus orca*)," J. Acoust. Soc. Am. **122**, 1365–1373.

Vincent, A. C. J., and Sadler, L. M. (**1995**). "Faithful pair bonds in wild seahorses, Hippocampus whitei," Anim. Behav. **50**, 1557–1569.

Volodina, E. V., Volodin, I. A., Isaeva, I. V., and Unck, C. (**2006**). "Biphonation may function to enhance individual recognition in the Dhole, *Cuon alpinus*," Ethology **112**, 815–825.

Wilden, I., Herzel, H., Peters, G., and Tembrock, G. (**1998**). "Subharmonics, biphonation, and deterministic chaos in mammal vocalization," Bioacoustics **9**, 171–196.

Zimmer, W. M. X. (**2011**). *Passive Acoustic Monitoring of Cetaceans* (Cambridge University Press, Cambridge, UK), pp. 124–127.

Zollinger, S. A., Riede, T., and Suthers, R. A. (**2008**). "Two-voice complexity from a single side of the syrinx in northern mockingbird *Mimus polyglottos* vocalizations," J. Exp. Biol. **211**, 1978–1991.

TABLE I. Summary of multifractal spectrum related shape parameter $\Delta h(q)$. Normally, the exponent $h(q)$ will depend on q. For q=2, the Hurst exponent H in standard detrended fluctuation analyses (DFA) could be retrieved. The subtle difference in $h(2)$ values apparently shows the similarity with the second-order Hurst exponent or power-law exponent associated with the clicks [The second-order Hurst exponent account for the overall root-mean-square (RMS) fluctuation in the data].

Seahorse	Clicks	$h(2)$	Click $\Delta h(q)$	Surrogate $\Delta h(q)$
12 cm female	1	–0.816	0.752	0.366
	2	–0.698	0.746	0.220
	3	–0.645	0.724	0.231
	4	–0.653	0.740	0.209
	5	–0.800	0.704	0.226
12 cm male	1	–0.711	0.592	0.111
	2	–0.722	0.613	0.180
16 cm male	1	–0.862	0.385	0.179
	2	–0.629	0.420	0.144
	3	–0.843	0.319	0.183
	4	–0.829	0.349	0.175
	5	–0.771	0.363	0.171
	6	–0.624	0.439	0.165
	7	–0.675	0.338	0.117
	8	–0.609	0.424	0.176
18 cm male	1	–0.774	1.101	0.169
	2	–0.686	1.022	0.214
	3	–0.695	0.979	0.298
	4	–0.781	0.896	0.321
	5	–0.746	0.918	0.304

FIGURE CAPTIONS

FIG. 1. (Color online) An example of the oscillogram and the corresponding spectrogram of 12 cm female seahorse clicks after filtering are depicted in panel (a) and (b). The passive acoustic signals are recorded using a hydrophone. The inset in panel (a) shows the temporal variation of the local Hurst exponent Ht in the first click. The computation of Ht is advantageous to identify the time instant of structural changes within the time series (Ihlen, 2012). The spectrogram analyses reveal phase couplings in the feeding clicks with several dominant frequencies (ranging between 1 kHz–5 kHz). The phase coupling behavior essentially necessitates the application of MFDFA to characterize the multifractality of the click, as illustrated in panel (c) and (d). In panel (c) the generalized Hurst exponent $h(q)$ corresponding to the third click and the background noise is compared. The $h(q)$ values are calculated using Eq. (4). Similarly, the multifractal spectrum $f(\alpha)$ [computed using Eq. (6)] is displayed in the panel (d). The comparison of $h(q)$ and $f(\alpha)$ spectrum reveal the multifractal behavior of the feeding click, but the background noise indicates a non-multifractality.

FIG. 2. (Color online) Graphical representation of signal extraction methodology. The oscillogram of 12 cm female seahorse clicks after filtering is depicted in panel (a). Panel (b) shows a zoom in on the small scale, indicating the intermittent amplitude variation along with the background noise. The background noise in the analyses will generate spurious multifractality. Accordingly, the precise duration of the clicks is identified employing a noise level reduction method [panel (c)] and envelope detection procedure [panel (d)]. After identifying the time window [panel (d), dashed line], the corresponding amplitude values of each click is extracted from the data stream illustrated in panel (a). The extracted noise-free clicks are subjected to MFDFA to verify the existence of long-range power-law correlation in the data.

FIG. 3. (a) Log-log plot of the fluctuation function $F_q(s)$ in the feeding click of 12 cm female, with respect to the segment sample size s for selected q values. Panel (b) shows the schematic representation of the generalized Hurst exponent $h(q)$ used to compute the width value $\Delta h(q)$. In panel (c) the multifractal scaling exponents $\tau(q)$ corresponding to the click is compared with a typical monofractal signal. The monofractal signal displays $\tau(q)$ with a linear q-dependency. The multifractal seahorse click indicates a curved q-dependency. Panel (d) depicts the resulting multifractal spectrum $f(\alpha)$ that can also be used to evaluate multifractality. The $h(q)$ and $f(\alpha)$ are mathematically related by the Legendre transformation. Hence, only the $\Delta h(q)$ values are assessed to determine the individual characteristics. The $F_q(s)$, $h(q)$, $\tau(q)$ and $f(\alpha)$ have been calculated using Eqs. (3), (4), (5) and (6) respectively.

FIG. 4. (Color online) Multifractality in seahorse feeding clicks. The ensemble average of the $h(q)$ values (18 cm male) corresponding to the feeding clicks and associated surrogates have been compared to validate nonlinearities in the data [panel (a)]. The surrogate series for the feeding clicks were generated by employing iterated amplitude adjusted Fourier transformation (IAAFT). The $\Delta h(q)$ of surrogate has smaller value as compared to the original time series, indicating significant influence of phase couplings across temporal scales in the data. In panel (b) the ensemble average of the generalized Hurst exponent $h(q)$ curve corresponding to the individual seahorse is exemplified. The shape of $h(q)$ curve for the individual is broad, indicating multifractal behavior. The highest degree of multifractality is evident in the 18 cm male seahorse. A relatively reduced multifractality and heterogeneity can be observed in the feeding clicks of 16 cm male seahorse. Note that the intercept point of the $h(q)$ curves for the individual is close to q=2. This intercept pattern reflects similarity in second-order Hurst exponent or power-law exponent (see Table I), and demonstrates a spectral *blind spot* identified by MFDFA (see text for more details). The second-order Hurst exponent account for the overall root-mean-square (RMS) fluctuation in the data.

FIG. 5. (Color online) Box plot represents the variability of the multifractal spectrum related shape parameters $\Delta h(q)$ in the seahorse feeding clicks and associated surrogates. The illustration of the shape parameter is shown in Fig. 3b. The box in the figure represents the central 50% of the data. Its lower and upper boundary lines are at the 25% and 75% quantile of the data. The dashed line indicates the median. The two horizontal lines (below and above the box) demarcate the remaining data points outside the box that are not regarded as outliers.

FIG. 6. (Color online) Panel (a) and (b) illustrates the comparison of $\Delta h(q)$ and second-order Hurst exponent $h(q=2)$ with respect to seahorse body size. The corresponding weight values are displayed in the Panel (a), and regions of individual clicks are clearly delineated. The second-order Hurst exponent values in Panel (b) have been calculated from the $h(q)$ curves for q=2. The identical and subtle variations in $h(q=2)$ are caused by the spectral *blind spot* identified by MFDFA.

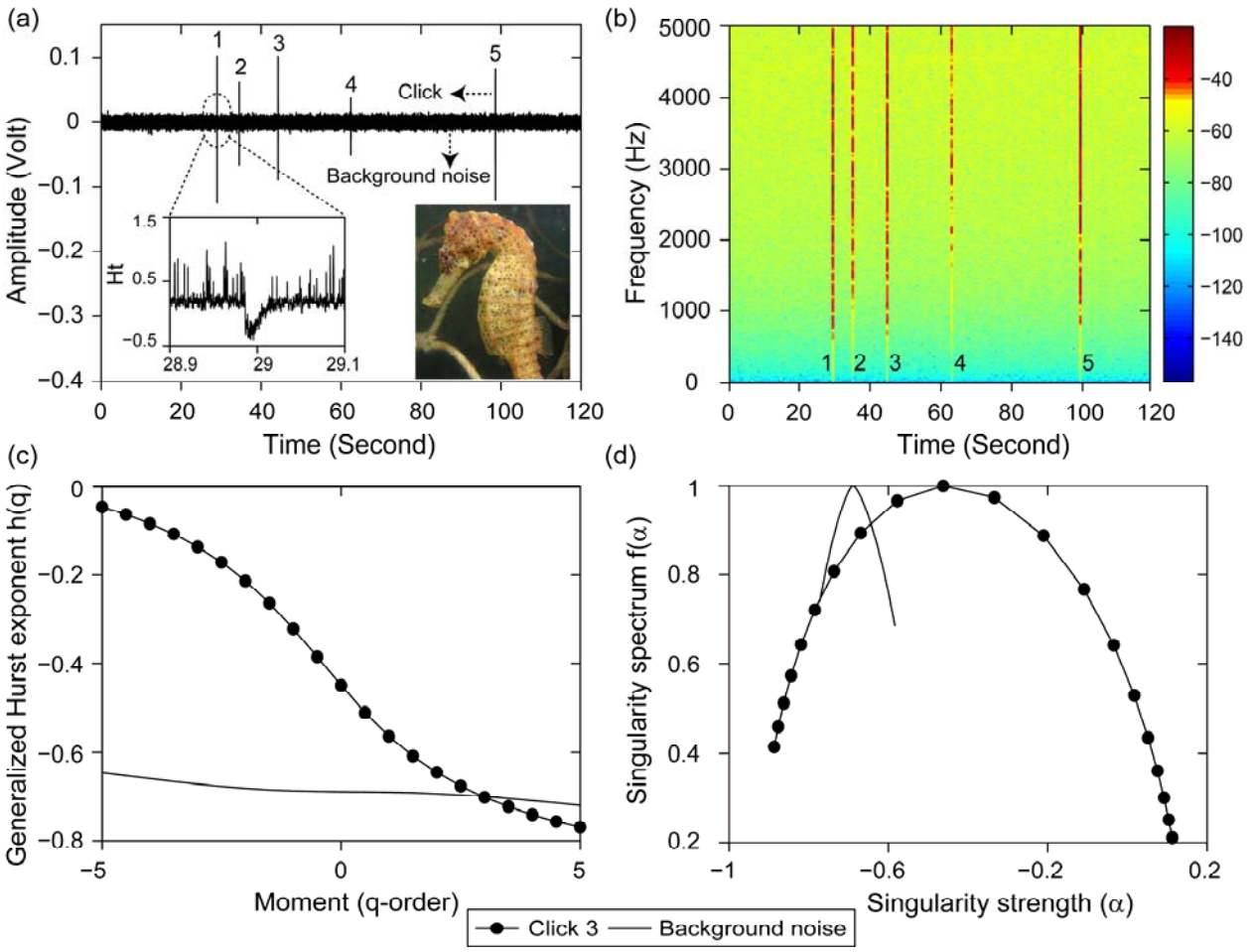
(a)
Amplitude (Volt)
Time (Second)
Click
Background noise
Ht
(b)
Frequency (Hz)
Time (Second)
(c)
Generalized Hurst exponent h(q)
Moment (q-order)
(d)
Singularity spectrum f(α)
Singularity strength (α)
Click 3
Background noise

FIG. 1.

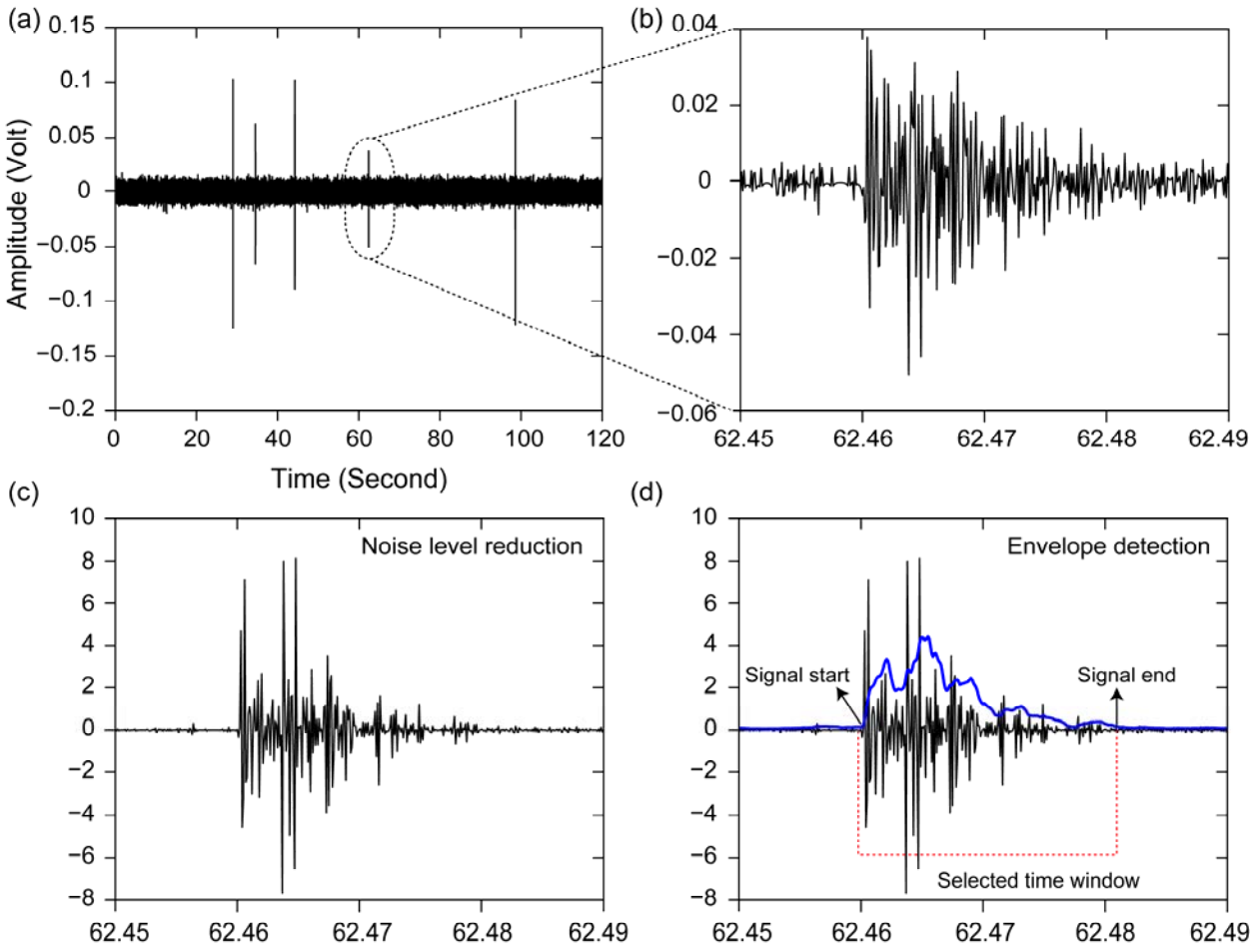
(a)
(b)
(c)
(d)
Amplitude (Volt)
Time (Second)
Noise level reduction
Envelope detection
Signal start
Signal end
Selected time window

FIG. 2.

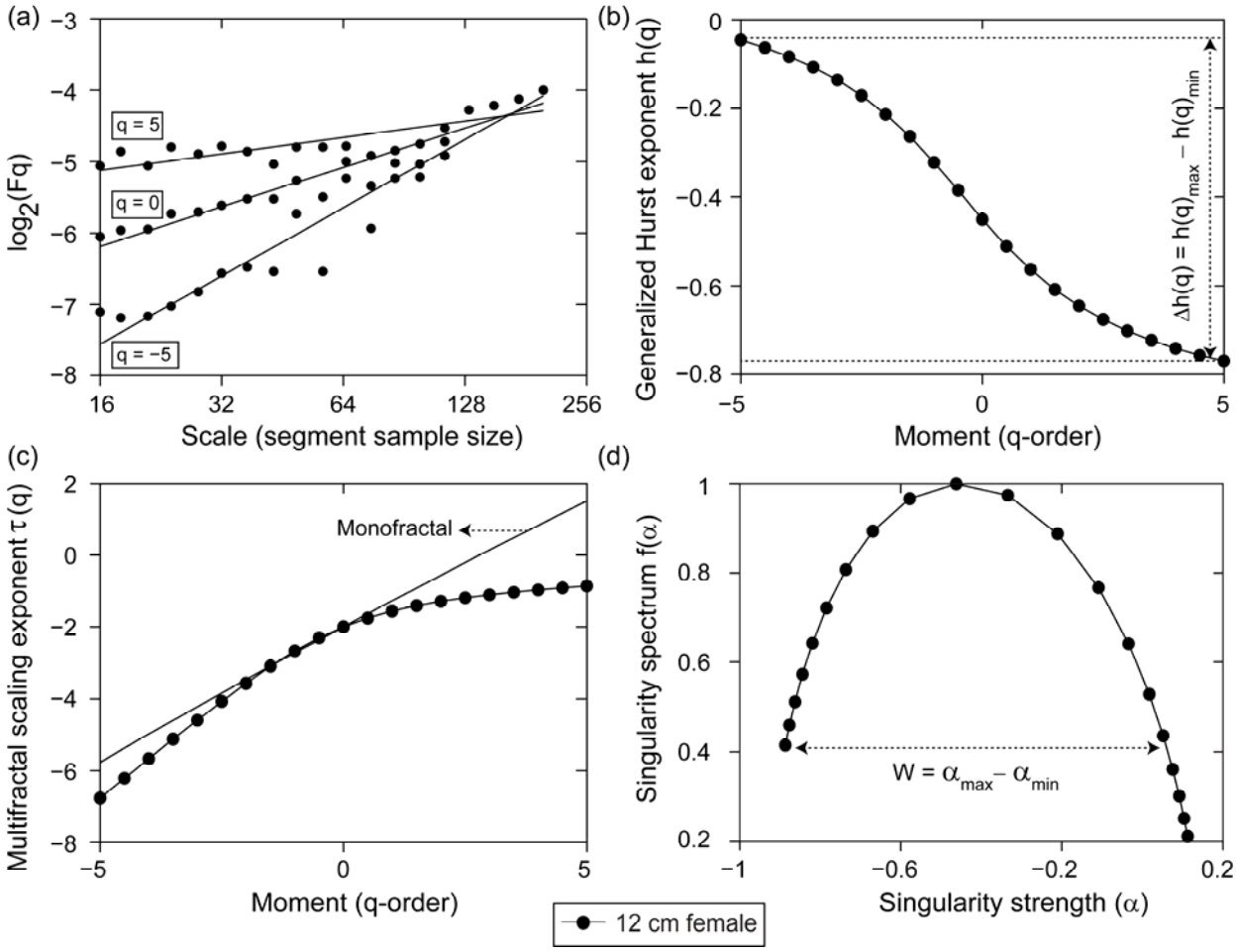
(a)
log2(Fq)
q = 5
q = 0
q = −5
Scale (segment sample size)
(b)
Generalized Hurst exponent h(q)
Δh(q) = h(q)max − h(q)min
Moment (q-order)
(c)
Multifractal scaling exponent τ(q)
Monofractal
Moment (q-order)
(d)
Singularity spectrum f(α)
W = αmax − αmin
Singularity strength (α)
12 cm female

FIG. 3.

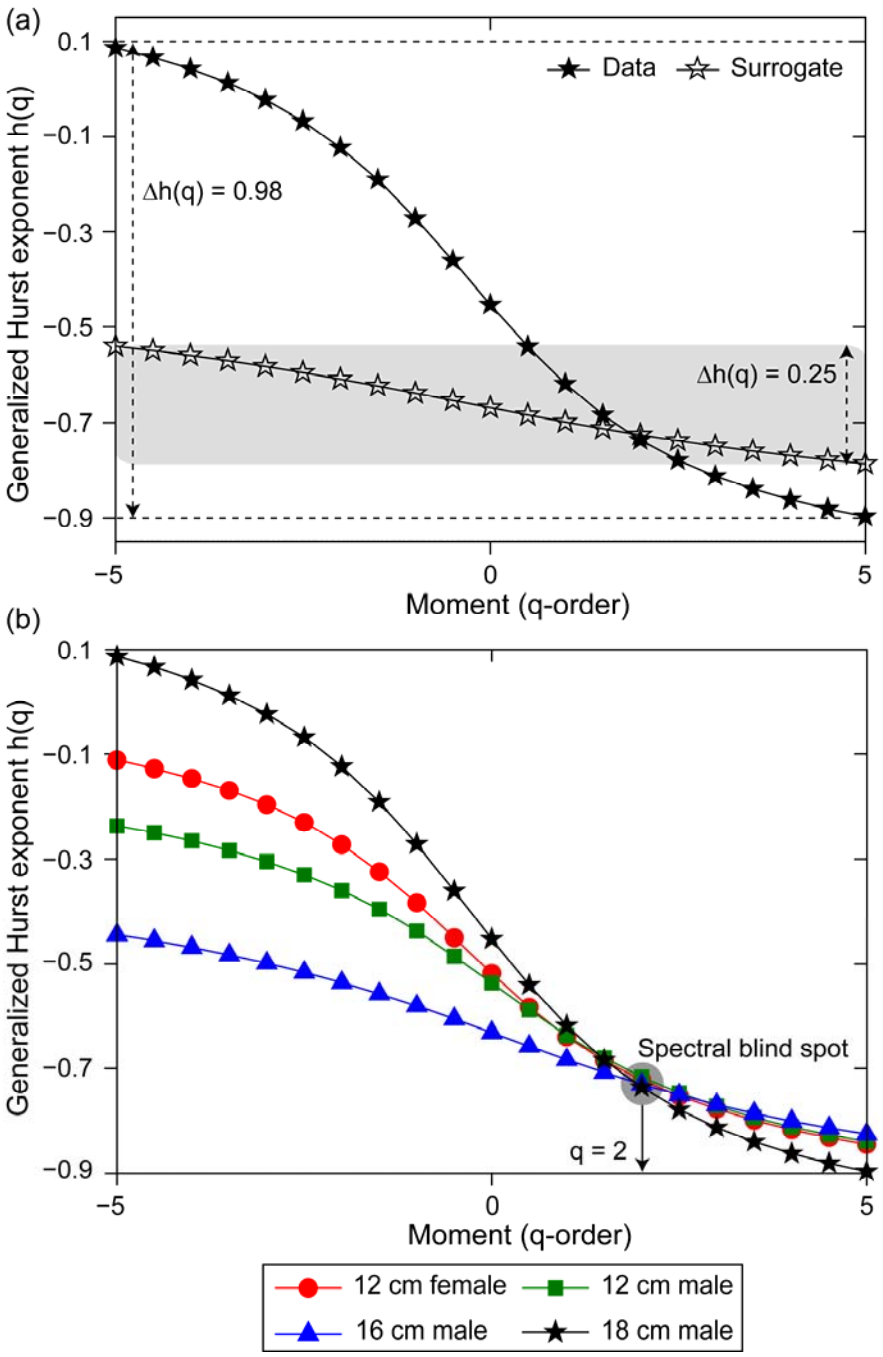
(a)
Data
Surrogate
Δh(q) = 0.98
Δh(q) = 0.25
Generalized Hurst exponent h(q)
Moment (q-order)
(b)
Spectral blind spot
q = 2
12 cm female
12 cm male
16 cm male
18 cm male

FIG. 4.

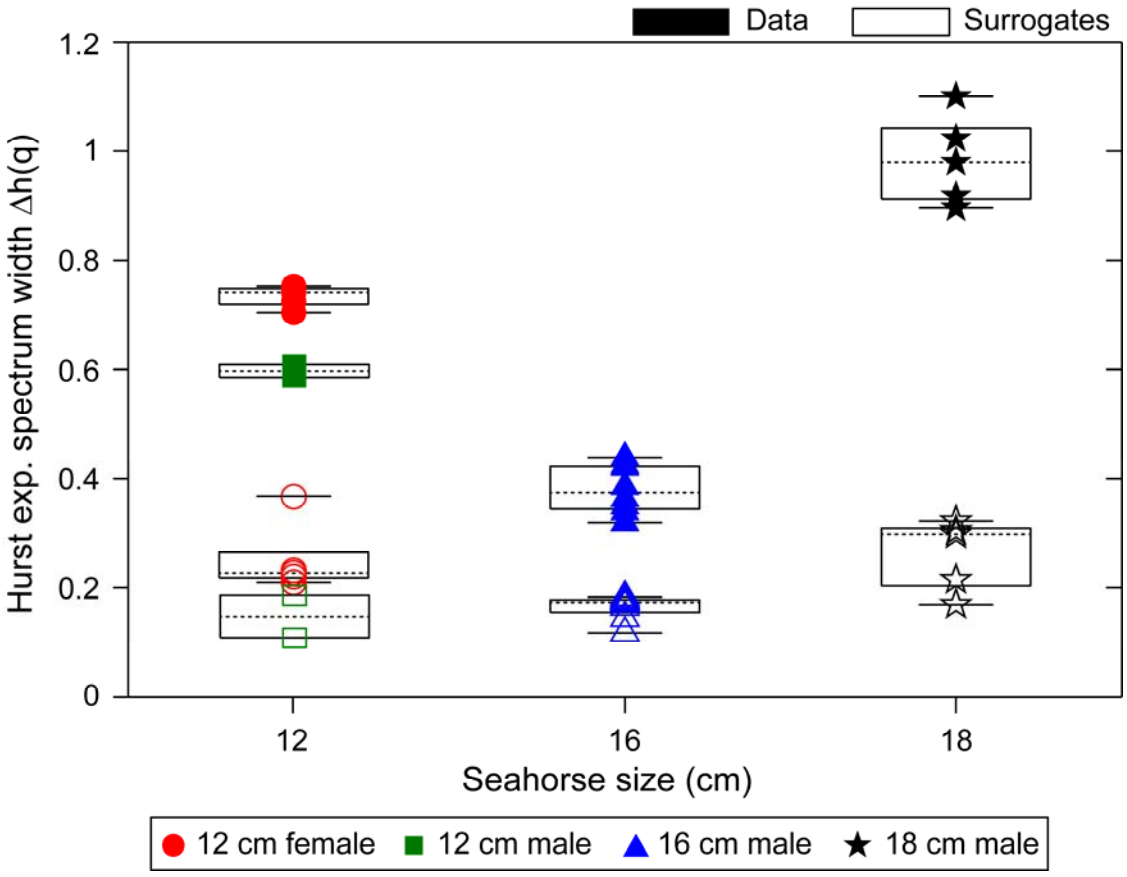
Data
Surrogates
Hurst exp. spectrum width Δh(q)
1.2
1
0.8
0.6
0.4
0.2
0
12
16
18
Seahorse size (cm)
12 cm female
12 cm male
16 cm male
18 cm male

FIG. 5.

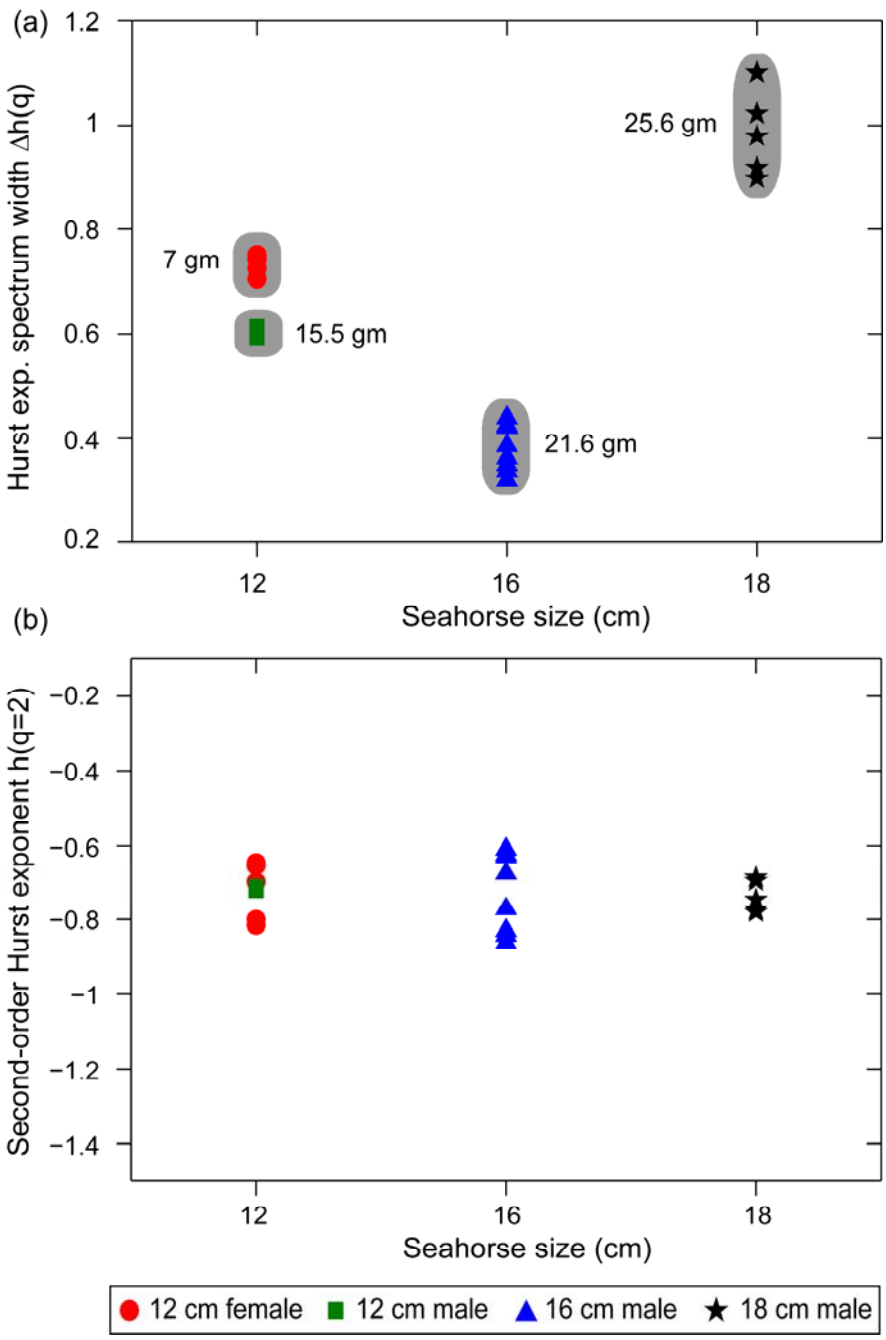
(a)
Hurst exp. spectrum width Δh(q)
1.2
1
0.8
0.6
0.4
0.2
7 gm
15.5 gm
21.6 gm
25.6 gm
12
16
18
Seahorse size (cm)
(b)
Second-order Hurst exponent h(q=2)
−0.2
−0.4
−0.6
−0.8
−1
−1.2
−1.4
12
16
18
Seahorse size (cm)
12 cm female
12 cm male
16 cm male
18 cm male

FIG. 6.